scientific reports

Check for updates

OPEN

The perceptual and biomechanical effects of scaling back exosuit assistance to changing task demands

Jinwon Chung[1,3]✉, D. Adam Quirk[1,3], Jason M. Cherin[1], Dennis Friedrich[1], Daekyum Kim[1,2] & Conor J. Walsh[1]✉

Back exoskeletons are gaining attention for preventing occupational back injuries, but they can disrupt movement, a burden that risks abandonment. Enhanced adaptability is proposed to mitigate burdens, but perceptual benefits are less known. This study investigates the perceptual and biomechanical impacts of a SLACK suit (non-assistive) controller versus three controllers with varying adaptability: a Weight-Direction-Angle adaptive (WDA-ADPT) that scales assistance based on the weight of the boxes using a chest-mounted camera and machine learning algorithm, movement direction, and trunk flexion angle, and standard Direction-Angle adaptive (DA-ADPT) and Angle adaptive (A-ADPT) controllers. Fifteen participants performed a variable weight (2, 8, 14 kg) box-transfer task. WDA-ADPT achieved the highest perceptual score (88%) across survey categories and reduced peak back extensor (BE) muscle amplitudes by 10.1%. DA-ADPT had slightly lower perceptual (76%) and peak BE reduction (8.5%). A-ADPT induced hip restriction, which could explain the lowest perceptual score (55%) despite providing the largest reductions in peak BE muscle activity (17.3%). Reduced perceptual scores achieved by DA and A-ADPT were explained by controllers providing too much or little assistance versus actual task demands. These findings underscore that scaling assistance to task demands improves biomechanical benefits and the perception of the device's suitability.

Back exos, including exoskeletons and exosuits, have been developed to reduce the risk of occupational low back injuries (LBI)[1]posed by tasks with high peak and cumulative lumbar moments[2–4]. Engineering controls designed to reduce lumbar moments, such as adjusting table height and installing electric hoists, have demonstrated reductions in LBI rates[5]. Given that back exos effectively reduce back extensor (BE) moments and muscle activity[1], they could mitigate the risk of developing occupational LBIs[6,7]. However, devices must have a high intention to maximize this potential[8].

In the workplace, the adaptability of back exos is crucial due to the diverse range of manual material handling tasks involved, such as bending, lifting, transferring, and walking[9,10]. A practical approach to support bending and lifting tasks involves adapting assistance based on the trunk flexion angle, which elicits a proportional increase in back extensor moment[11–13]. Consequently, numerous passive and active exos assist using angle adaptive (A-ADPT) controllers, effectively reducing back extensor moments and muscle activity as measured by electromyography (EMG)[14–17]. Although scaling device assistance to a simple stiffness function is effective, it poses biomechanical and perceptual challenges when a user performs tasks outside the device's intended use case, such as deep flexion or walking[1,9,18–20]. To prevent burdens, users must select a stiffness and engagement angle that provides robust lifting assistance while minimizing assistance delivered during unintended or incompatible tasks that can oppose their motion[21,22]. Research indicates that the increased assistance provided by higher stiffness devices can lead to greater reductions in agonist (i.e., back extensor) muscle activity during lifting and lowering tasks[15,22,23]. However, this approach can result in increased co-activation of antagonist muscles and may lead to a reduced range of motion (RoM)[15,23,24], especially during periods where one moves in opposition to device-related assistive forces[22,25,26]. From a perceptual standpoint, the forces exerted by higher stiffness devices can increase the sensation of movement restriction or device discomfort in the shoulders, chest, and hips during lifting, bending, walking, and lowering activities[18,23,24,27]. Careful consideration of these perceptual impacts

[1]John a. Paulson School of Engineering and Applied Sciences, Harvard University, Boston, MA, USA. [2]School of Mechanical Engineering, Korea University, Seoul, South Korea. [3]Jinwon Chung and D. Adam Quirk contributed equally to this work. ✉email: jinwon.chung16@gmail.com; walsh@seas.harvard.edu

is crucial, as negative perceptions of exos can significantly diminish a worker's motivation to use exos in the workplace[9,28,29].

To minimize burden, there is growing interest in leveraging automatic clutch technology or active exos to adapt to task demands. To date, active exo controllers are becoming increasingly sophisticated, recognizing and delivering assistance to varying activity states[13,20,30,31], or proportional to estimated changes in task demands (i.e., external moments)[32,33]. Increasing device adaptability can improve biomechanical effectiveness[33,34], which benefits back exos. For example, disengaging device assistance to a swing leg during walking can preserve gait kinematics and economy[20], leading to reduced perceived burden[30]. Furthermore, many active back exos provide lower assistance during trunk flexion and higher assistance during trunk extension[35–38]. These direction-adaptive (DA-ADPT) controllers can result in individuals selecting higher peak assistance (virtual stiffness) when lifting than with a fixed stiffness impedance approach[39]. This enables DA-ADPT controllers to reduce peak BE muscle activity comparable to a high-stiffness angle adaptive (A-ADPT) passive system during lifting while minimizing the perception of discomfort and movement restriction associated with the A-ADPT during lowering[23]. Despite these benefits, the DA-ADPT controller approach is limited by its inability to adapt to the load on hand. Specifically, this approach accepts the trade-off of less restriction during flexion at the expense of reducing biomechanical effectiveness when lowering heavy objects[14,20,23,40].

It is widely recognized that lumbar moments increase proportional to the mass of a lifted object[12,14,41]. Consequently, providing the same level of assistance for objects of different masses can lead to assistance discrepancies, which can be perceived as insufficient or excessive support[14,22,25]. Additional controller adaptation to object weight could overcome the limitations of direction-angle adaptation (DA-ADPT) approaches. Previous studies have explored various techniques, such as using cameras, pressure gloves, electromyography (EMG), or inertial measurement unit (IMU) sensors placed on the back, arms, or legs to detect whether a wearer is holding an object or scaling assistance proportional to increased effort[12,16,30,31,42–46]. These more complex controllers, if employed accurately, provide biomechanical benefits over angle adaptive approaches[20,30,42,43]. However, less is known about whether scaling assistance to task demands can improve the perceptual factors that drive exo acceptance[8,47].

Despite their potential to improve device compatibility, weight-adaptive controllers have not been deployed long-term in the field[8,10,48]. This is partially explained by inter-subject variability, model errors, and sensor noise, which could affect the accuracy of estimating tasks or object weight, leading to robustness or safety issues[10,12,20,43,49–51]. Provided angle adaptive and direction-angle adaptive controllers represent a robust state-of-the-art approach in the field[8,10,48], there is a need to demonstrate improvements in effectiveness from more adaptive controllers to encourage technology acceptance[52].

This study aimed to investigate the perceptual and biomechanical effects of three controllers with varying degrees of adaptability: a Weight-Direction-Angle adaptive (WDA-ADPT) controller, a Direction-Angle adaptive (DA-ADPT) controller, and an angle adaptive (A-ADPT) controller. As part of our investigative procedure, the WDA-ADPT controller was specially developed for this study, incorporating robust weight adaptation through a chest-mounted camera monitoring user activity. In a proof-of-concept scenario, a machine-learning model was trained to identify the weight of various objects within a highly controlled lab environment. For each controller, participants engaged in a highly dynamic variable weight transfer task, which involved lifting, transferring, and lowering different colored boxes of varying weights (Fig. 1). To establish a baseline comparison, we included a SLACK (non-assistive) condition, where a minimal tension of 10 N was applied. For consistency, we selected the gains of all controllers to match the peak forces during the weighted extension phase once averaged across different weights. These four conditions were compared using a blocked randomized order (Figure S1). Throughout the experiment, we collected data on muscle activity, kinematics, kinetics, and perceptual surveys (Table S1–3) to gain comprehensive insights into the impacts of these different controllers, testing the hypothesis that while consistent with previous work DA-ADPT will improve device perception over an A-ADPT controller at the expense of reduced biomechanical effectiveness, a WDA-ADPT could provide biomechanical and perceptual benefits to a DA-ADPT approach.

Results

Weight-direction-angle adaptive (WDA-ADPT) controller

The WDA-ADPT controller applies assistance via two principles. First, it delivers assistance asymmetrically by scaling down the assistance during trunk flexion based on past findings, which show that higher peak lowering forces can be more restrictive and uncomfortable[23], while scaling up assistance during trunk extension. Second, it scales assistance based on the impact of object weight on the overall lumbar moment[23]. In particular, the suit delivered ~ 12.5% of the estimated peak hip extensor moment when lifting and 7.8% when lowering. As a proof-of-concept study, we trained a machine-learning model (Fig. 2B, details in the method section) that infers the user's holding state and recognizes color-coded boxes of different weights (2 kg: yellow, 8 kg: orange, 14 kg: red) using images from a camera mounted on the chest strap. By incorporating the classification outcome, the WDA-ADPT controller applied different force profiles for three weights. Figure 2 A depicts the overall system flow and the force profiles while lifting and lowering the three weights.

The classification algorithm for the WDA-ADPT controller quickly (within 15 ms) and accurately (99% accuracy) identified the holding state and the object type classification on the test set of the image data collected for training the model. During the variable weight transfer experiment, participants performed 540 lifts using the WDA-ADPT controller (15 participants x 12 reps x 3 weights). Out of 540 lifts, only two lifts (0.4%) were misclassified, defined as when the flexion gain and the extension gain were not set as intended based on the movement and the object's weight (details in the method section). For those two misclassified lifts, it was found that the chest strap occluded the camera.

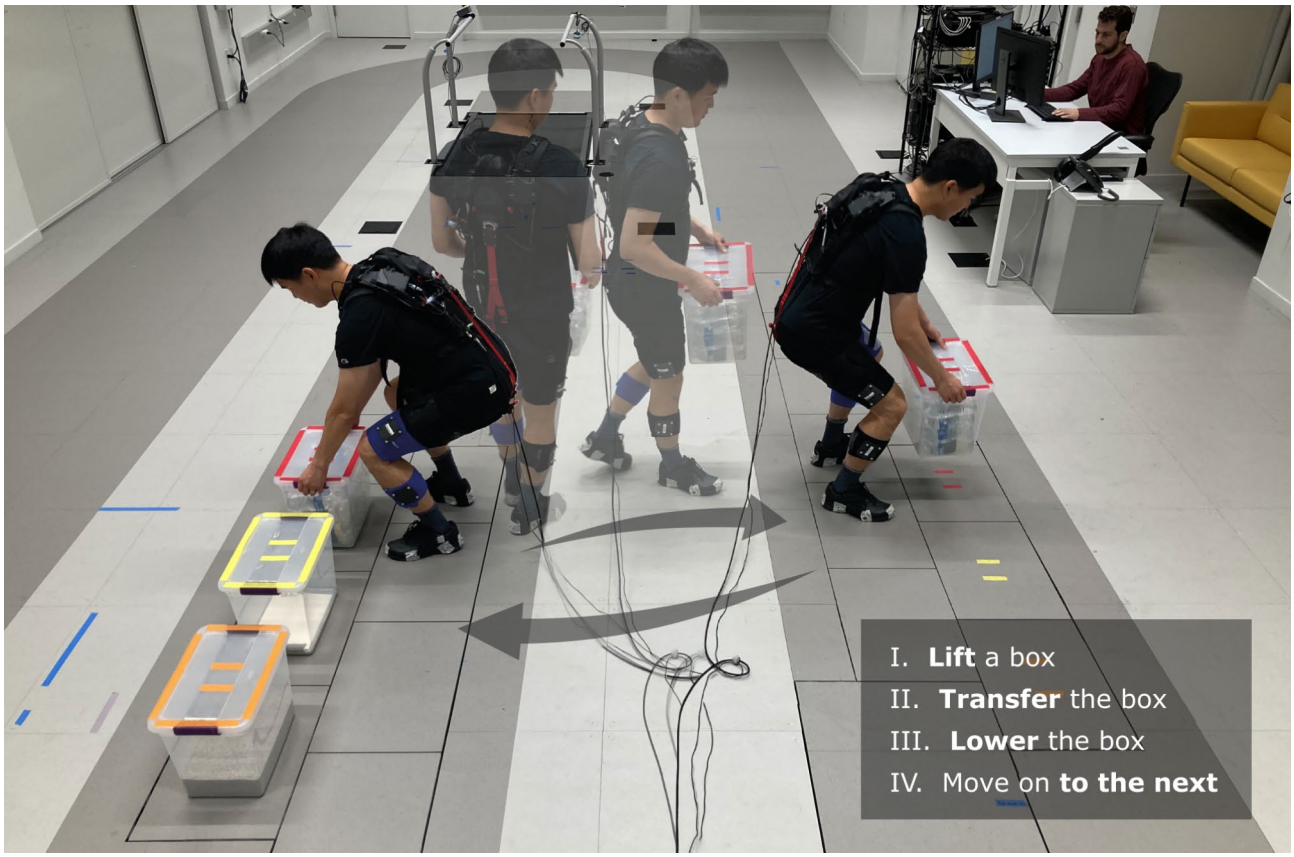

Fig. 1. Variable weight transfer experiment protocol. Participants followed a sequence of steps listed in numerical order. Participants would lift the box in front of them, transfer it to the colour-coordinated marked spot on the floor, lower it, and then move on to the next box.

Assistance profiles

Descriptions of A-ADPT and DA-ADPT controllers are in the methods. Figure 3 illustrates that each controller applied different peak and median forces for different object weights during the lifting and lowering phases (Tables S4&5), with minimal peak and median error between the device's force command and measured load (Tables S6&7). As intended, WDA-ADPT successfully applied different peak force profiles depending on the object's holding state and weight when lifting and lowering (Fig. 3A&B). When averaged across weights, the peak forces delivered during the weighted extension phases were similar (within 9 N) between all assistive controllers (Table S4 & Fig. 3C). In contrast, peak forces varied considerably (up to 122.3 N) in other lifting phases (Table S4).

The median forces among controllers were different. As intended, both DA-ADPT and WDA-ADPT applied lower force during the unweighted (Fig. 3C) and weighted flexion (Fig. 3D) when compared to extension (Table S5). Consistent with the controller function, both DA-ADPT and WDA-ADPT delivered less median assistance than A-ADPT during weighted extension, in part due to the interpolation method used to smoothly transition assistance based on direction (flexion to extension state) (Table S5 and Fig. 3D). Hence, once averaged across all lifting phases, WDA-ADPT and DA-ADPT delivered significantly lower median forces than A-ADPT (Fig. 3E), designed to deliver consistently high median assistance across all moment phases (Fig. 3C&D & Table S5). Differences in median controller assistance were not uniform across all lifting phases and varied most between controllers during weighted flexion. By inferring object weight, WDA-ADPT applied 49.2% higher median assistance than DA-ADPT, whereas A-ADPT applied approximately 89.3% higher median assistance than DA-ADPT during weighted flexion (Table S5 & Fig. 3D&F).

Controller impacts on participant perception

After completing the variable weight transfer task under each condition, participants were asked to respond to three categories of questions: those assessing positive attributes, the absence of negativity, and weight-specific performance. For simplicity, we computed an overall survey score by aggregating the individual survey scores (calculation details in the method section) to evaluate the overall perceptual impact. Based on the results, WDA-ADPT was rated as the top-performing controller (88%), followed by DA-ADPT (76%) (Fig. 4A, Table S1). A-ADPT received the lowest score (55%) among the three controllers, a score that was nearly as low as the SLACK condition (43%) (Table S1).

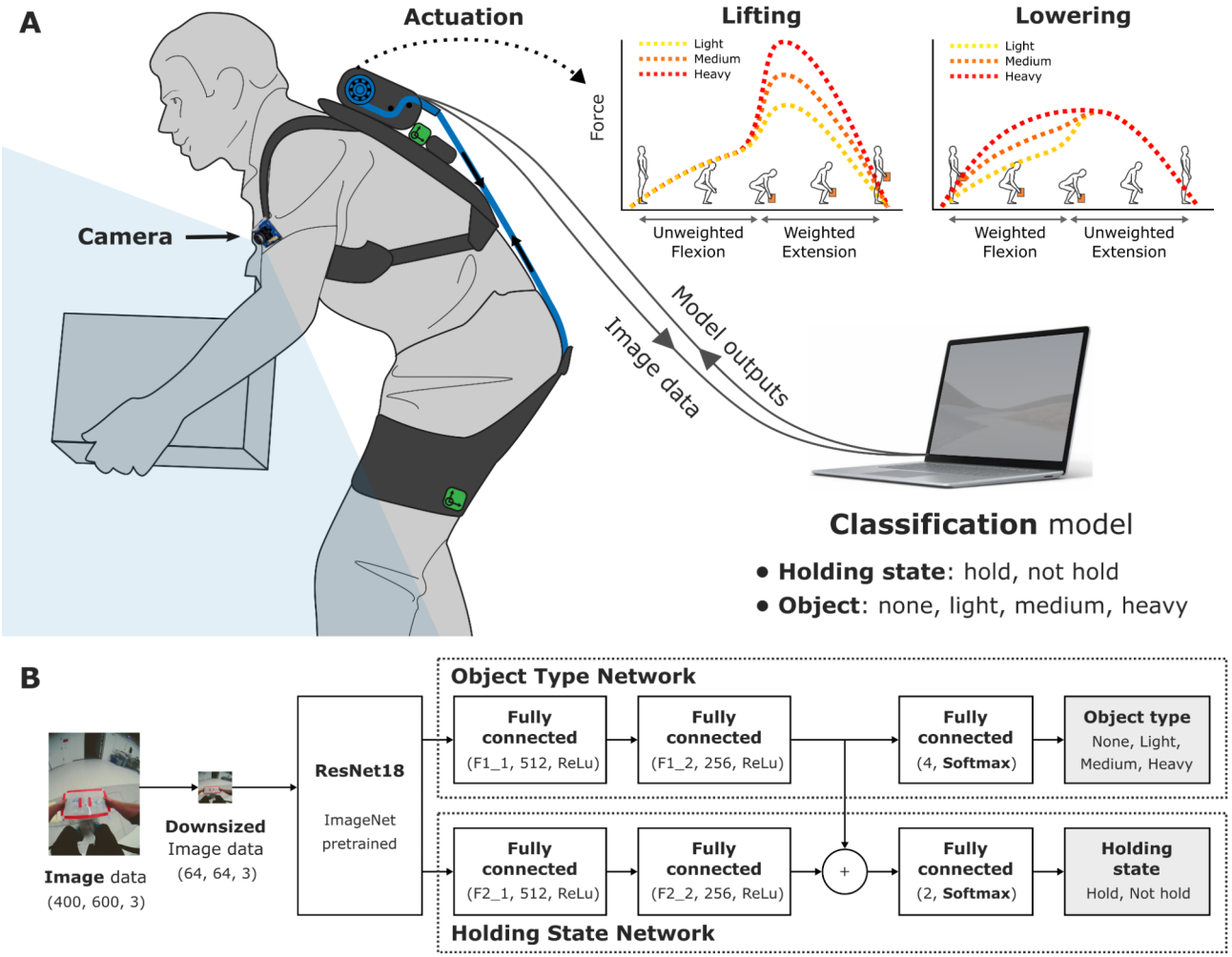

Fig. 2. Weight-Direction-Angle adaptive (WDA-ADPT) controller. (**A**) Overview: The camera captures image data that is then transferred to the connected laptop. The classification model running on the laptop identifies the task using the image data by recognizing the holding state (whether the participant is holding an object) and the object (light, medium, heavy, or no object). Based on the model outputs, the controller generates the force profiles shown in the upper right corner. (**B**) Model architecture: The model takes downsized image data as input to estimate the object type (None, Light, Medium, Heavy) and holding state (Hold, Not Hold). The image in sub-plot A has been modified using an image from a previous work by the original authors[36].

To interpret the overall score, we analyzed survey scores within the three perceptual categories (Fig. 4B). Considering positive attributes (Fig. 4B Top), WDA-ADPT and DA-ADPT received higher scores than A-ADPT (Table S1). Across the spectrum of the three weights (Fig. 4B Left), participants were most satisfied with WDA-ADPT and the least satisfied with A-ADPT (Table S2). Analyzing the frequency of negative attributes (Fig. 4B Right), WDA-ADPT had the fewest instances of perceptually negative events (high scores). Meanwhile, A-ADPT elicited the most negative events (Table S1). Specific, negative perception depended on the controller type (Figure S2). The SLACK condition offered too little assistance. A-ADPT was generally considered too restrictive, and depending on object weight, both DA-ADPT and A-ADPT were considered too jerky and delivered too much assistance, especially when interacting with the lighter box (Figure S2 and Table S3).

Interactions between controller assistance and object mass on perception

The secondary analysis sought to probe whether controller perceptions depended on the weight of the object that participants interacted with. It was found that the perception of controller suitability was dependent on weight. Both positive (Table S2) and negative attributes (Table S3) demonstrated weight by controller interactions. While WDA-ADPT maintained a favorable impression regardless of weight, DA-ADPT and A-ADPT induced more negative perceptions when participants interacted with light-weight objects than heavier-weight objects (Fig. 5). As one might expect, aside from the perception of providing too little assistance, especially when lifting a heavier mass, the SLACK condition had minimal negative attributes at the expense of eliciting minimal perceived benefits (Table S2 & S3).

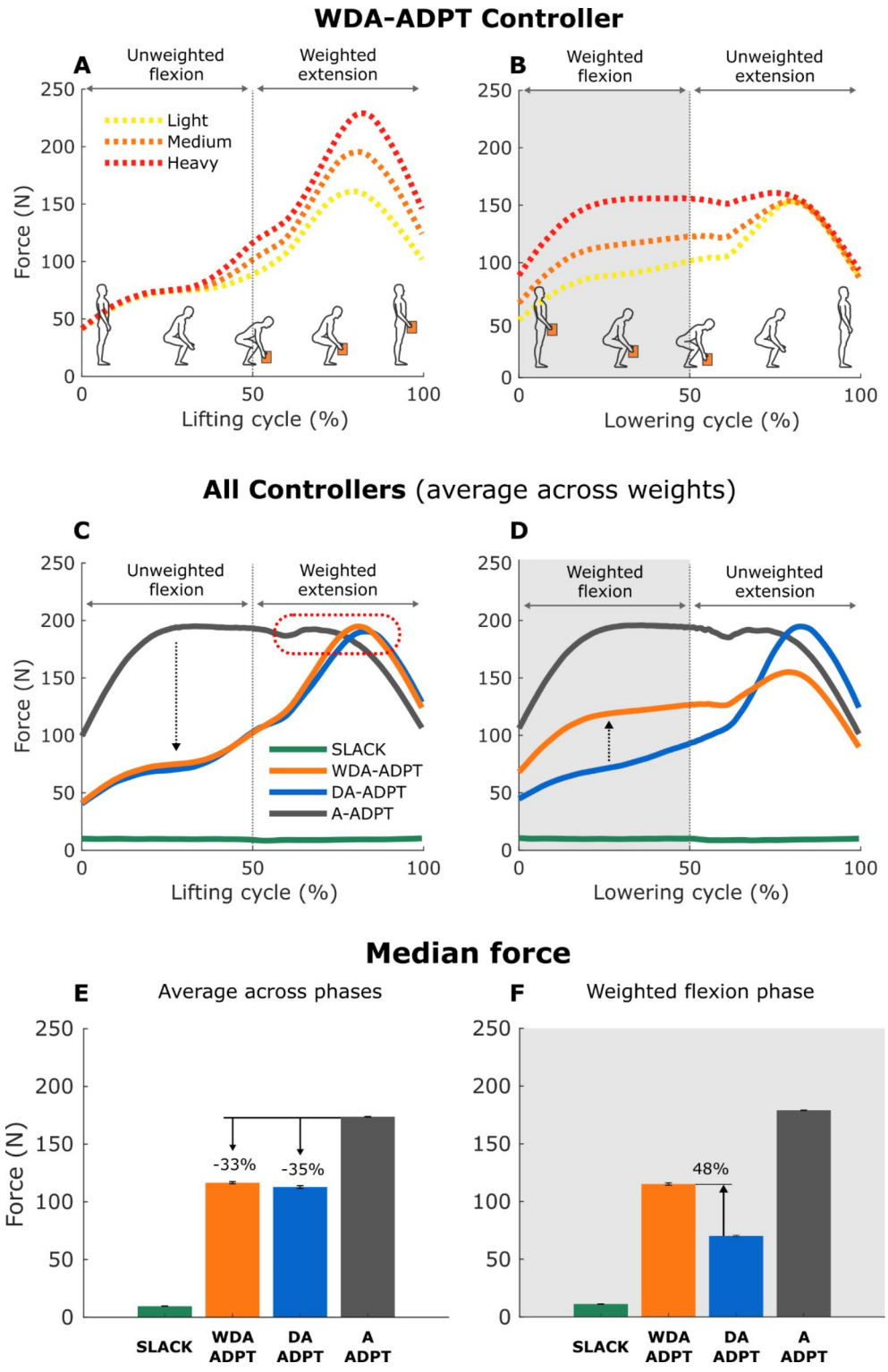

Fig. 3. Force profiles and median force of the controllers. Subplots **A** & **B** portray the ensemble average force profiles of WDA-ADPT for three different weights throughout the lifting and lowering cycles. Subplots **C** & **D** portray each controller's ensemble average force profiles once averaged across weights throughout the lifting and lowering cycle. Arrows highlight that A-ADPT applied higher forces than other controllers during the unweighted flexion (**C**), and WDA-ADPT generated higher forces than DA-ADPT during the weighted flexion (**D**). The dotted oval in weighted extension (**C**) indicates that the three controllers achieve similar peak forces. Subplot **E** presents the median forces of each controller across all four phases, and subplot **F** shows median forces within the weighted flexion (grey shading) to portray significant mass by phase by controller interactions. All error bars reflect standard error.

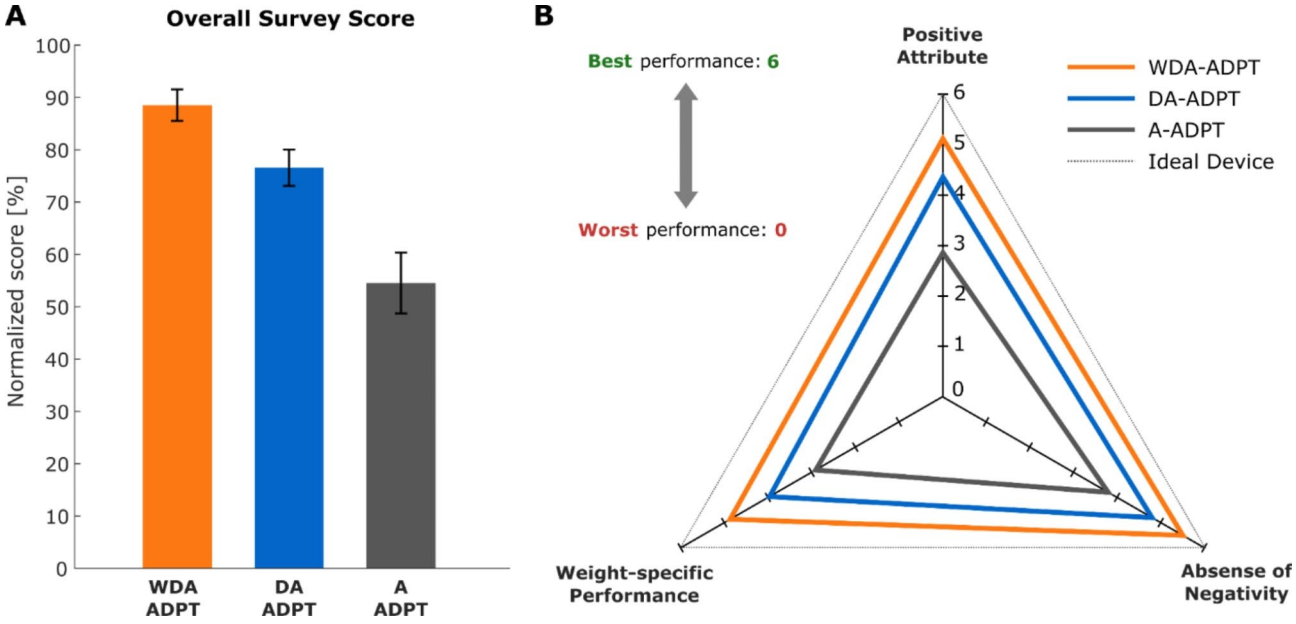

Fig. 4. Perceived controller performance. Subplot **A** shows the normalized overall survey score across the three assistive exosuit controllers. This composite score is computed by aggregating the individual survey scores obtained from all the questions during the protocol. Error bars represent standard error. Subplot **B** highlights average scores in three perceptual categories across three exosuit controllers (positive attribute, absence of negativity, and weight-specific performance). The gray dotted line depicts the ideal score. Slack suit survey scores were left out as the device was not assistive with the SLACK controller.

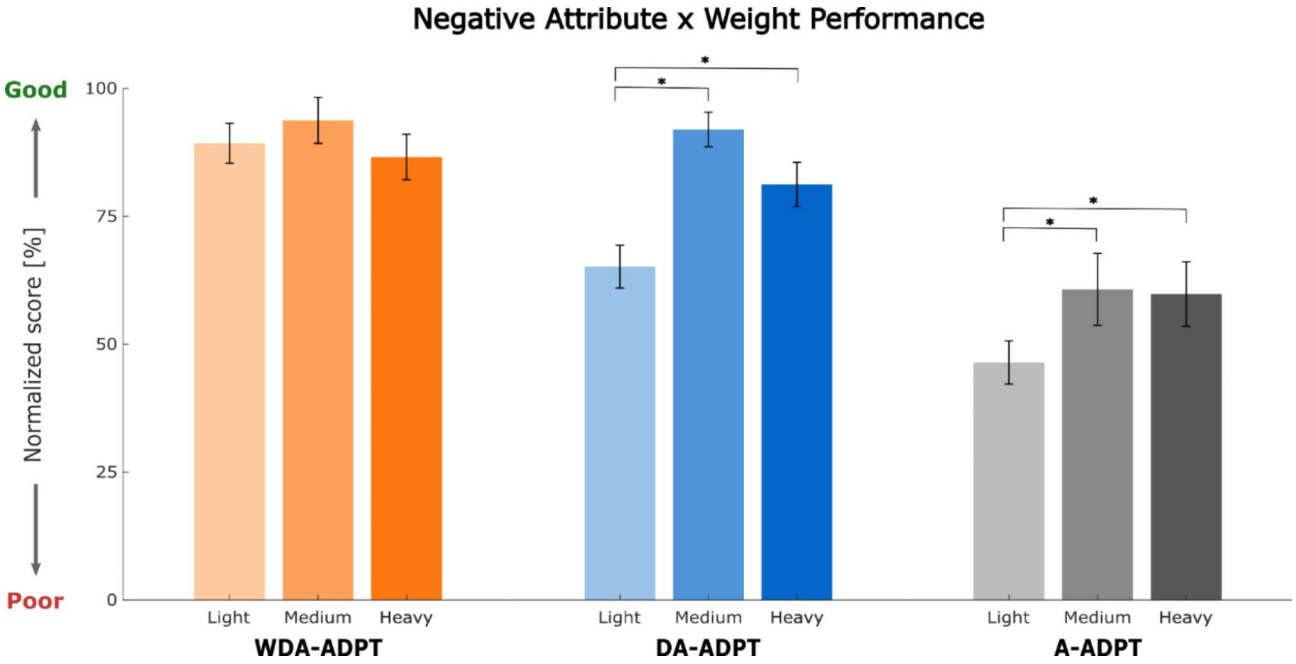

Fig. 5. Negative Attribute by Weight Performance Interaction. This plot highlights the changes in controller performance based on questions surrounding negative controller attributes (too much or too little assistance, jerkiness, and restriction) when lifting a specific box (light, medium, and heavy). The asterisk (*) denotes a significantly greater score for the medium and heavy boxes than for the light box. Error bars represent standard error.

Controller impacts on EMG and biological moments

When averaged across all movement phases and weights, the peak back extensor EMG was reduced by WDA-ADPT (10.1%), DA-ADPT (8.5%), and A-ADPT (17.3%) when compared to the SLACK condition (Fig. 6A & Table S8). For median back extensor activity, a controller-by-phase interaction captured WDA-ADPT decreased median amplitudes to a greater extent than DA-ADPT during the weighted flexion phase (Fig. 6B & Table S9). However, DA-ADPT and WDA-ADPT achieved similar reductions during the other phases. This finding was corroborated by controller-by-phase interactions in the analysis of biological lumbar moments (Table S10&11). Compared to SLACK, WDA-ADPT (6.2%) reduced biological lumbar moments more than DA-ADPT (5.8%) during the weighted flexion phase. Consistent with load cell data, A-ADPT (11.9%) minimized peak biological extensor moments the most (Table S10). Similar results were reported in the analysis of median biological lumbar moments (Table S11).

Controller impacts on secondary biomechanical outcome measures

As for the secondary biomechanics outcome measures, peak and median abdominal EMG amplitudes did not change when exposed to different controllers (Table S12&S13). This suggests that there is no controller induced antagonist muscle co-activation. Considering other kinetic and kinematic measures (Tables S14-S19), the A-ADPT controller reduced hip flexion motion by up to 1.05° compared to WDA-ADPT and SLACK conditions (Table S17). All assistive controllers increased ankle dorsiflexion by up to 1.55° compared to SLACK (Table S19). No controller differences were found for lumbar or knee flexion (Tables S16 & 18). These small kinematic differences did not influence peak overall lumbar moments (Table S14). However, median overall lumbar moments were significantly lower (up to 3.3 Nm or 2.4%) for the A-ADPT controller compared to WDA-ADPT and DA-ADPT controllers (Table S15).

Auxiliary experiment: comparing angle adaptive (A-ADPT) controller with PASSIVE

We conducted an auxiliary experiment comparing the A-ADPT and DA-ADPT controllers to a true passive elastic (PASSIVE) controller in 6 participants to understand the biomechanical superiority of A-ADPT compared to the DA-ADPT (see supplementary material and Tables S20-S24). This auxiliary experiment showed that A-ADPT delivered more median assistance than PASSIVE (Table S21), explaining why A-ADPT achieved greater EMG reductions (Tables S22 & S23) and higher perceptions of restriction (Table S24) versus an authentic passive suit that achieved EMG reductions comparable to DA-ADPT.

Discussion and conclusions

The main objective of this study was to explore the perceptual and biomechanical effects of three assistive controllers with varying levels of adaptability when dynamically lifting external loads with variable mass. Consistent with our hypothesis, increasing device adaptability improved overall perceptual scores. In contrast, a more adaptive controller's biomechanical implications were less clear. The least adaptive A-ADPT exhibited the highest back extensor EMG reduction but received the lowest composite perceptual score. The most adaptive WDA-ADPT achieved the highest perceptual scores, simultaneously improving biomechanical performance compared to DA-ADPT. This discussion will highlight how context-aware wearable robots that scale assistance

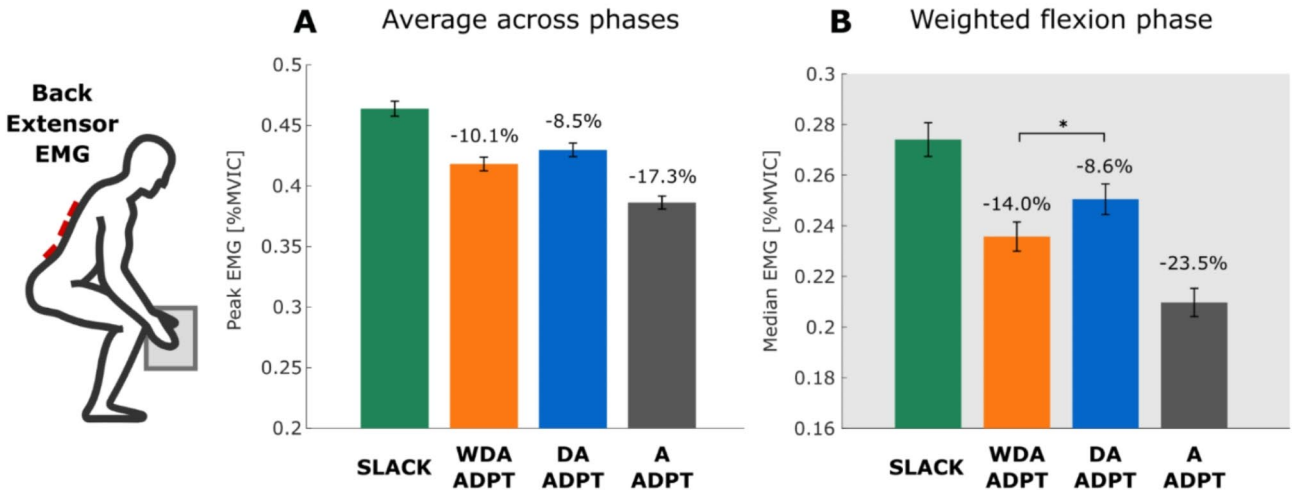

Fig. 6. Back extensor EMG averaged across phases and in the weighted flexion phase. Subplot **A** shows that all three controllers significantly reduced peak back extensor EMG average across all phases compared to SLACK. Subplot **B** portrays a significant reduction in median back extensor EMG within the weighted flexion phase across all three conditions compared to SLACK. The asterisk (*) in subplot **B** highlights a more significant EMG reduction of WDA-ADPT than the DA-ADPT, during the weighted flexion phase. The percentages on both subplots represent the percent difference to the SLACK condition, while the error bars reflect the standard error.

to task demands could improve the ability of industrial exos to provide greater assistance without perceptual burdens.

Impact of device adaptability on controller perception

To encourage adoption, a back exo should be compatible with the operator, allowing an individual to complete tasks with minimal perceptions of movement restriction, disruption, or device discomfort[9,29,52]. Comparing perceptual scores across controllers, we revealed that more adaptive controllers were generally considered more compatible, particularly when scaling device assistance to task demands.

The angle adaptive (A-ADPT) controller was the least adaptive and exhibited similarities to passive anti-gravity assistance profiles[11,53,54]. While the A-ADPT approach can reduce task-related effort[1], it often delivers excessive assistance forces (Table S3), potentially leading to increased discomfort, movement restriction, and job disruptions[22,23,25,54]. More recently, it has been shown that device incompatibility, arising from too much assistance, could depend on movement direction. In particular, delivering assistive moments in opposition to a user's intended direction increases local interaction forces[22], and antagonist co-activation[22,25,55], as users may oppose forces to maintain vigor[56]. However, other factors also contribute to the perception of incompatibility[29]. Using state thresholding, exos can adaptively scale assistance based on movement direction, similar to a DA-ADPT controller[35–37,39], thereby providing less assistance during flexion and increased assistance during extension. These controllers strive to maintain or increase the amount of positive work a device offers while limiting the delivery of negative work to mitigate some perceptual burdens associated with an A-ADPT approach (Table S1)[23].

In this study, we corroborated that a direction-angle adaptive (DA-ADPT) controller provides perceptual improvements over angle adaptation (A-ADPT) alone[39], reducing restriction to near-ceiling levels (score of 5.3/6 Table S1(Q4))[23]. Direction-angle adaptation (DA-ADPT) had additional benefits, reducing the perception that DA-ADPT applied too much assistance, as noted with A-ADPT (Table S1 Q1). This finding suggests that individuals might be more sensitive to the higher median force delivered by A-ADPT than DA-ADPT (Table S5 & Fig. 3C&D). Given the lower median assistance provided by DA-ADPT, especially during lowering, it was more likely to be perceived as delivering the right assistance, improving a user's satisfaction with the device, and intention to use (Table S1Q6-8) versus A-ADPT. Yet these improvements did not reach a perceptual ceiling (scores of 3.8–4.7/6) because controller effectiveness interacted with object weight. When lifting a 2 kg mass, both DA and A-ADPT were perceived to provide too much support, disrupting the participants' motion (Table S3 Q12&14). Meanwhile, these controllers were perceived to provide too little support for a 14 kg mass (Table S3 Q13). Previous studies have shown that individuals are more likely to accept higher device assistance for more demanding tasks[22,25,54]. Our current study shows that reduced negative perceptions may explain this tolerance. Interestingly, A-ADPT received a lower negative composite score for light and medium-weight objects than the SLACK condition (Table S3). This result could suggest that unless the overall assistance of the A-ADPT controller was lowered, an individual could be inclined to disengage assistance, remove, or abandon a device to reduce these negative perceptions, despite perceptions that the A-ADPT controller was helpful for the heavy-weight object[54].

Comparing an A-ADPT with the DA-ADPT approach, one might surmise that delivering less assistance during flexion affords perceptual benefits. However, this study emphasizes a crucial interplay between assistance magnitude and task demands; hence, adding weight-direction-angle adaptation (WDA-ADPT) further increased composite perceptual scores (Table S1) and device compatibility. By reducing median assistance during 2 kg and unweighted extension by 20–24 N or ~ 14–15% compared to DA-ADPT (Table S5), WDA-ADPT significantly reduced the perception of being too assistive (Table S1 Q1). A finding that occurred even though WDA-ADPT increased net assistance versus DA-ADPT by 25 or 18% when lifting a 14 kg box and by 18–72 N or 25–104% for weighted flexion across the 2–14 kg mass, respectively (Table S5). Using a machine learning model to scale assistance for each object made transitions between flexion and extension smoother (Fig. 3C&D), reducing perceptions of jerk (Table S1 Q3). Provided that the increased assistance provided by WDA-ADPT paradoxically decreased perceptions of restriction compared to DA-ADPT (Table S1 Q4), WDA-ADPT made users perceive that the weight adaptive controller delivering the right assistance, indicated by increased user satisfaction and intention to use (Table S1Q6-8) to near ceiling levels (scores 5–5.2/6). Hence, these results align with theories of device compatibility and embodiment[57], suggesting that higher levels of assistance do not necessarily impose perceptual burdens, and if assistance is appropriately scaled to the operator's contextual demands, it can even enhance overall perception.

Biomechanical implications of increased device adaptability

Unlike perceptual results that revealed increased adaptability improved compatibility, biomechanical benefits and side effects depended on the overall magnitude of assistance each controller delivered. The angle adaptive (A-ADPT) controller exhibited the greatest reduction in back extensor activity and biological lumbar moment (Table S8 & S10) attributable to its higher median assistive force (Fig. 3C&D). This outcome aligns with prior studies indicating that increased assistance correlates with greater reductions in back extensor EMG activity[15,23]. Surprisingly, while it was anticipated that the direction adaptive (DA-ADPT) controller would provide smaller reductions to biological lumbar moments compared to the angle adaptive (A-ADPT) controller, especially during flexion (Table S10 & 11), the A-ADPT controller outperformed DA-ADPT in reducing peak back extensor EMG activity. This is notable given that previous studies have indicated similarities between DA-ADPT and passive assistance systems[23]. An auxiliary experiment highlighted that the angle adaptive (A-ADPT) controller significantly reduced back extensor muscle activity (15%) more than a true PASSIVE elastic (9.4%). This finding can be explained by A-ADPT applying 41% higher mean assistance than PASSIVE, achieved through mitigating

hysteresis and delivering more overall work by assisting trunk flexion with sinusoidal rather than a linear impedance function, increasing the device's effective bandwidth (see supplementary material)[23].

Regardless of the enhanced overall effectiveness of the A-ADPT controller, our goal of the adding weight adaptation (WDA-ADPT) was to improve the biomechanical benefits of the DA-ADPT so they would be closer to the A-ADPT without the associated perceptual burdens. Compared to DA-ADPT, the increased assistance delivered by WDA-ADPT during the weighted flexion did yield greater reductions for biological lumbar moments (Table S8) and median back extensor activity reductions (Fig. 6and Table S12), suggesting this strategy can improve the immediate biomechanical effectiveness of this controller strategy. The ability of WDA-ADPT to deliver the highest perceptually tolerated assistance during lowering could be biologically relevant since musculotendinous tissue damage is more likely to occur during eccentric (lowering) contractions[58,59]. Furthermore, the ability of WDA-ADPT to increase device perception may have implications for improving the long-term cumulative effectiveness of back exosuits by increasing the likelihood of wearing these devices for longer durations in the working day, even when compared to a DA-ADPT strategy[6,7].

It is important to acknowledge, despite variations in effectiveness, all three assistive controllers reduced peak back extensor EMG by 8.5–17.3%, which is standard for this back exosuit (12–18%)[23,36,60] and is typical for other back exosuits and exoskeletons (10–40%)[1]. However, in the present study, the 8.5% peak back extensor EMG reductions achieved by DA-ADPT is lower than in previous studies[23]. Reduced effectiveness in the current study could be attributed to the lower peak assistance (200 N) delivered by DA-ADPT in this study compared to previous studies (240 N). Higher peak exosuit assistance leads to greater back extensor EMG reductions[15,23]; hence, our results closely match the 8–11.5% reductions obtained by a passive device that delivered comparable peak assistance (180 ± 50 N)[23]. Further reductions in effectiveness can be explained by the fact that participants in this study exerted higher peak back extensor moments (195–200 Nm) than previous work (175–185 Nm)[23]. These increases in task moments were likely explained by the lower vertical box position and variable horizontal box position during the unconstrained movements in this study, which diminished device effectiveness if a back exo delivers fixed assistance[14,16].

Considering biomechanical side effects, no antagonist co-activation was observed (Table S12&13), but all assistive controllers subtly increased ankle dorsiflexion by 1.5° compared to the SLACK device control. Additional biomechanical side effects were found for the angle adaptive (A-ADPT) controller, including restricted hip movement and reduction in the median overall lumbar moment (Table S15&17). These data suggest that higher assistance during flexion might lead to physical movement restriction. Exosuit-induced kinematic alterations, although capable of minimizing lumbar moments[61], can pose a risk of overloading unintended joints[15], and disrupt natural movement patterns, which, although subtle, can be perceived negatively[1,62]. Despite biomechanical subtleties, the limited kinematic alterations observed with direction (DA-ADPT) and weight adaptive (WDA-ADPT) controllers might explain why they were perceived favorably compared to A-ADPT. This suggests that consistent with other studies, the perception of a device may be incongruent if biomechanical benefits simultaneously elicit kinematic and kinetic deviations that hinder the sense of device embodiment[8,23,29].

Study limitations

This study has some limitations. First, it was designed as a proof-of-concept study in a laboratory, and the technology needs to be further developed for use in the field. To succeed in the field, the machine learning model must be trained using various objects in complex environments[43]. Also, the model should be further optimized to implement a mobile GPU without tethering to a laptop. However, if this approach was included in an embedded system, an optical-based mass estimate would likely be occluded if objects were placed in a generic box. Thus, the results of this study provide that there could be a perceptual value added in emerging approaches, including adding force (insoles or pressure), EMG, or IMU sensors to estimate lumbar moments or object payload if implemented with low error[12,33,41,42,50,51,63]. To date, new exo controllers are emerging, which either scale assistance using binary classification of mass in hand[16,31], or proportional to estimated hip or lumbar moments[13,32,33,42]. Our current study did not use these strategies as we attempted to develop a proof-of-concept study that maximized robustness. While not explored in the current study due to time constraints, future work should consider the extent of the benefit provided if a system delivers assistance using graded or continuous strategies, such as the method in this strategy, versus a discrete event (mass in hand), as this study demonstrates a simple discrete solution (DA-ADPT) can provide considerable perceptual benefits. Regardless of this limitation, a strength of this study was to demonstrate there is viability in pursuing new methods to scale device assistance to task demands.

Second, both direction-angle adaptive (DA-ADPT) and angle adaptive (A-ADPT) controllers used a generic profile that delivered peak assistance that would be approximately 15.5% (range 12.5–20.8%) of the peak hip extensor moment that occurred during unweighted flexion and extension of a hypothetical (1.72 cm and 73 kg) individual lifting a 6 kg mass. For simplicity, the same generic gains were used for all participants. Given that conventional anthropometric-based scaling approaches tune devices to deliver around at most 20% task moment[27,42,54,64], these generic profiles should not be considered too assistive for most individuals, especially as lumbar moments increase when lifting a heavy object (Table S10, 11, 14 & 15). Future work must determine if optimal parameter settings can be found based on calibrating around participant anthropometry and changing task demands[26,65]. Finally, we elected to have each controller strategy normalized to deliver comparable magnitudes of peak assistance. However, if our A-ADPT controller used our lower generic gain of 80 N, both the DA and WDA-ADPT controllers would likely show adaptation and demonstrate biomechanical benefits similar to other studies that use a generic profile of an object with the lightest weight[42,43]. While we would hypothesize a lower bound (80 N) A-ADPT controller would be less restrictive, all other perceptual changes, including intention-to-use, are unknown. Regrettably, this condition could not be tested in the present study due to data collection time constraints.

Conclusions

By utilizing a proof-of-concept WDA-ADPT controller to quickly (15ms) and accurately (99%) identify object mass during dynamic tasks, this study provides new insight into the benefits of adapting exosuit assistance to task demands (object weight and movement direction). In particular, consistent with previous work, minimizing assistance upon lowering with a DA-ADPT approach improved overall perceptual scores (76%) over typical gravity assistance A-ADPT controller (55%) at the cost of eliciting a reduction in median back extensor EMG that was 2.3–2.4 times lower than it's A-ADPT counterpart. However, using a WDA-ADPT strategy that increases device adaptation was shown to improve perception (88% overall score) despite increasing overall lowering assistance by 25–104% to enhance to improve median back extensor EMG reductions by 1.5–1.9 when compared to this DA-ADPT strategy. These findings suggest that if deployed robustly, increased controller adaptation can afford biomechanical and perceptual benefits, paving the way for future ambulatory wearable robotic systems capable of sensing and adapting to changing task contexts as a solution to increase intention to use.

Materials and methods

WDA-ADPT controller development

Hardware configuration

The back exosuit used in this study (Fig. 2), as described in previous publications[23,36], can apply force up to 250 N using the ribbon cable-driven actuation. It has three inertial motion sensors (IMUs) that capture movements of the back and the thighs at 100 Hz. We installed a camera (ELP-USB2MP; Shenzhen Ailipu Technology Co., Ltd, Shenzhen, China) on the chest strap of the back exosuit to collect images in front of the user (Fig. 2) at 100 Hz using a wide 180° fisheye lens. The image data was sent to a laptop (Eluktronics MAX-15; Newark, USA) running the detection algorithm. The classification results were fed back to the exosuit via wired CAN communication to update the force commands.

Detection algorithm

We used a machine learning approach to classify (i) holding state (i.e., whether a person is currently holding (H) or not holding (NH) an object), and (ii) object type (i.e., light, medium, or heavy box) the person is about to hold or is holding using an image at time t. To train the model, six participants (2 Females, 30.2 ± 5.8 years old, 170 ± 11 cm, 72.2 ± 13.4 kg) performed two repetitions of the variable weight transfer task, which involved lifting and transferring three boxes of different weights (light 2 kg, medium 8 kg, and heavy 14 kg) (see Fig. 1). During this task, the exosuit applied negligible tension (10 N), while camera and force plate data were collected at 100 Hz and 200 Hz, respectively. All participants were screened for general health and were provided with and signed voluntary consent. This study was approved by Harvard Medical School's Internal Review Board (IRB 18–0960).

Data processing and labeling for detection algorithm

The collected image and force plate data were time-synchronized. For our transfer task, participants would hold and immediately lift a weight off the ground; thus, soon after participants held a weight, the normal force measured by the force plate under the object would lower below 10% of its recorded static weight. We used this event to label the holding state as Hold (H). Participants would return the object to another force plate without dropping the mass. When the force plate registered normal forces 95% of the object weight, we labeled the holding state as Not Hold (NH). Object types were labeled by manually drawing a bounding box for each object and finding the object that had the largest bounding box size. Each participant completed 12 trials; we used data from ten trials for training and two for testing our machine learning model.

Model development

In this study, we utilized an image-based machine learning model to predict the holding state (Hold, Not hold) and object type (None, Light, Medium, Heavy) at each time frame. The model was designed to operate faster than the short latency trunk muscle reflex response time of 33 Hz[66]. We used an image at every time frame to predict the holding state (Hold, Not hold) and the object type (None, Light, Medium, Heavy). The architecture of the model is illustrated in Fig. 2B. First, the images were downsized to $64 \times 64 \times 3$ and then fed into a ResNet18 convolutional neural network (CNN), which is widely used for object classification[67]. The ResNet18 model was pre-trained on ImageNet data[68]. The output of the ResNet18 was then input into the Object Type Network and Holding State Network. The Softmax activation function was applied to the final layer of each network to obtain probability distributions over the classes. The model was trained using the Adam optimizer with a mini-batch size of 16, a learning rate of 0.001, and a weight decay of $1e^{-6}$. The training was performed using an NVIDIA GTX1080 (Santa Clara, USA). The model was running on a laptop (Eluktronics, Newark, USA) equipped with an NVIDIA GTX3080 for real-time operation during the experiment.

Controller integration

During piloting, we found that the classification results for the holding state can be unreliable for a short transition phase from Not Hold to Hold or vice versa, as it can even be ambiguous to the human eye. Even a few misclassifications at this transition could apply uncomfortable forces to a user if we set the flexion gain and the extension gain at each time frame by directly using the holding state and the object type. To avoid this, we set the gains based on the holding state and the object type obtained at the beginning of the trunk flexion phase (passing 12° trunk flexion angle). For example, if an object type is a heavy box and a participant doesn't hold it at the beginning of the flexion phase, the flexion gain (75 N) and the extension gain (245 N) was set for this lifting cycle since participants predictably performed lifting and lowering tasks following the protocol described in the following section.

Variable weight transfer experiment

The goal of the variable weight transfer experiment was to investigate the biomechanical efficacy and the perceptual impact of three exosuit controllers with different levels of adaptability. During each trial of the main experimental blocks, participants completed six repetitions of the variable weight transfer task, described in the result section, using one of the three controllers or the SLACK condition described in the following section. Each main block consists of four controller conditions presented in pseudo-random counter-balanced Latin square order (Figure S1). Following condition randomization, participants completed two main blocks of each controller delivered in a fixed randomized order to mitigate any learning or fatigue effects and accommodate the re-appraisal of survey questions.

Controllers

Selection of controller gains

In this study, we evaluated the performance of three different controllers. For comparison between controllers, peak gain (referred to as GAIN, LIG, or LOG) during the extension phase (Fig. 3C) of the lift cycle was set such that all controllers would deliver assistance that was approximately 12.5% or 15% of the estimated hip or back extensor moment produced by a generic 1.72 cm and 73 kg individual handling a 6 kg mass with their trunk flexed at 90° and their shoulder flexed 10°. A static model was developed to estimate hip extensor moment when handling objects of different mass. Segment lengths, mass, and center of mass were estimated using standard anthropometric Table[69]. Object mass was modeled as a weight vector acting at the hand center of mass. These equations estimated that lifting a 6Kg mass would produce a hip extensor moment of 188.5Nm, similar to those measured using dynamic approaches (183-196Nm)[23]. Thus, all controllers were set to deliver 200 N of peak extension assistance, assuming a moment arm length of 12 cm (Table 1), once averaging across the different weights handled in our main experiment (0, 2, 8, and 14Kg)[23,70].

Walking adaptation

All adaptive controllers delivered assistance proportional to changes in trunk relative angle (θ), defined as $\theta = \theta_{Trunk} + 0.5\,(\theta_{RT} + \theta_{LT}) - 12° - 0.3\,\mathrm{abs}(\theta_{RT} - \theta_{LT})$, with θ_{Trunk}, θ_{RT}, and θ_{LT} representing the flexion angles of the trunk, right thigh, and left thigh in the sagittal plane, respectively. This approach ensured the exosuit delivered minimal assistance during walking to reduce movement restriction[20,36].

Angle adaptive (A-ADPT) controller

The A-ADPT controller was designed to represent a standard stiffness-based gravity assist controller, delivering assistance proportional to changing trunk flexion angle as used by many passive systems (Fig. 3C&D)[16]. In particular, this controller applies forces (F) to the trunk based on a sine function of trunk flexion angle (θ) and peak desired exosuit gain (GAIN = 200) according to Eq. 1 below.

$$F(\theta) = GAIN(\sin\theta) \tag{1}$$

Direction-angle adaptive (DA-ADPT) controller

The DA-ADPT controller, as shown in previous studies[23,36], refines the sine-based gravity assistance controller strategy by considering movement direction. In particular, this controller includes lower bound assistance defined by the device lowering gain (LOG) set to 75, which has been shown not to restrict trunk flexion for unweighted deep flexion tasks[23]. To scale assistance to movement direction, this controller considers trunk angular velocity ($\dot{\theta}$) within ± 120°/s. When an individual is flexing at 120°/s $q(\dot{\theta}) = 0$ and only LOG assistance is provided. However, when the participant extends greater than 120°/s $q(\dot{\theta}) = 1$and the participant experiences a GAIN defined by LIG 200 (Fig. 3C&D). To maintain a smooth and robust transition within the limits of ± 120°/s, the coefficient q was bounded between 0 and 1 using a quadratic interpolation[36], as seen in Eq. 2 below.

$$F(\theta, \dot{\theta}) = LOG(\sin\theta) + q(\dot{\theta})\,(LIG(\sin\theta) - LOG(\sin\theta)) \tag{2}$$

Weight-direction-angle adaptive (WDA-ADPT) controller

The WDA-ADPT controller described in Fig. 3A&B and Eq. 3 delivered assistance proportional to relative trunk angle and task direction similar to DA-ADPT, with additional gain scaling defined by holding state (where kg = 0 is No Hold), and our ML estimate of weight held in hand (kg = 2, 8, or 14 kg). For this controller, a state machine adjusted LIG such that the exosuit delivered assistance that was approximately 12.5% of the estimated hip extensor moments calculated using our static anthropometric model. Two criteria defined LOG; when the participant did not hold a mass, LOG was set to 75, comparable to our DA-ADPT controller. However, once mass was in hand, LOG was scaled such that the controller delivered assistance that was 7.8% of the estimated hip extensor moments using the gains listed in Table 1 and Eq. 3 below.

$$F(\theta, \dot{\theta}, kg) = LOG(m)(\sin\theta) + q(\dot{\theta})\,(LIG(m)(\sin\theta) - LOG(m)(\sin\theta)) \tag{3}$$

Slack controller

Finally, we also included a SLACK controller that did not consider trunk angle but kept constant tension (10 N) to hold the exosuit ribbon cable close to the body as a baseline (non-assistive) comparison.

Mass (kg)	Extensor moment (Nm)	LIG (*N*)	LOG (*N*)
0	155	160	75
2	165	170	105
8	200	210	130
14	235	245	160

Table 1. Estimated extensor moments when lifting a range of mass, and corresponding lifting gain (LIG), and Lowering gain (LOG) in newtons (N). Note that the gains and moments are rounded to the nearest 5 N.

Participants

Participants were recruited via local advertisement and word of mouth. Participants were generally healthy, free of neurological conditions, and back or neck pain in the last 6 months. Prior to data collection, all participants were provided with and signed voluntary consent approved by Harvard Medical School's Internal Review Board (IRB 18–0960). Participants, such as those in Fig. 1, separately provided informed consent to share photos or video recordings for presentations and publications. All protocol tasks, survey questions, setup, and collection methods followed protocol-specific guidelines and regulations. Fifteen participants (10 Men, 5 Women, 26 ± 6.1 years old, 178 ± 11 cm, 72 ± 11.8 kg) volunteered for this study. Missing EMG data are identified by corrected N in the supplementary tables. As a result of user error, one participant did not advance the survey appropriately, resulting in an inability to synchronize survey data with study tasks.

Study protocol

Upon arrival, the participants were equipped with electromyography (EMG) and inertial measurement unit (IMU) sensors. Following a structured study protocol (Figure S1), the participants performed two lifts of each box weight for a warmup with all four device controllers.

After the warmup, participants performed eight maximum voluntary isometric contraction (MVIC) tasks to target relevant muscle groups. A HUMAC dynamometer (CSMI, Stoughton, MA, USA) with a peripheral torso adapter was used to secure the participants in an approximately 15° trunk flexion position. Participants performed a warmup trunk flexion and extension to familiarize followed by two alternating maximal trunk extension and flexion. Afterward, participants performed a combined axial rotation, trunk flexion, and trunk extension task, first clockwise and then counterclockwise. Participants were instructed to ramp up and hold a maximum contraction for three seconds. Between repetitions, the participants had a 45-second recovery phase. Participants were prepared for motion capture and completed a static calibration before the familiarization block.

During the familiarization block, participants performed two repetitions of the variable weight transfer task to familiarize themselves with the device controllers and the task before the two main blocks. For each repetition, participants transferred three boxes (46 cm x 31 cm x 18 cm) in a fixed order (heavy, light, medium) from one side of the room to the marked position of the opposite side (Fig. 1). Each box transfer was initiated by a metronome signal every 12 s. After transferring all three boxes, participants returned to the heavy box and started the next repetition on a given signal. Although no specific lifting style was required, participants were encouraged to maintain a consistent lifting strategy throughout the experiment. Once completing all repetitions with a specific controller, participants were asked to complete a survey before repeating the previous steps with the next controller.

During the two main blocks, participants performed six repetitions of the variable weight transfer task using all three controllers and SLACK conditions dictated by their random order. Similar to the familiarization block, participants completed all survey questions (Tables S1-S3) upon completing six repetitions before proceeding to the next controller. After completing the block with all controllers, participants completed a post-block survey ranking controllers named arbitrarily in the order they were presented (1–4) to blind participants to the purpose and design of each controller.

EMG setup

Following standard skin preparation, surface bar electrodes (10 mm interelectrode distance) were positioned on five bilateral muscle sites following standard guidelines and minor adjustments based on palpation[23]. Six sensors were placed on the thoracic and lumbar erector spinae at the height of the T9, L3 (6 cm lateral to the 9th thoracic and 3rd lumbar spinous process), and L1 (3 cm lateral to the 1st lumbar spinous process) to capture the iliocostalis and longissimus fibers respectively. Four additional sensors were positioned on the upper rectus abdominis (URA) (3 cm lateral to the linea alba), and middle external obliques (EO) (15 cm lateral to the umbilicus oriented at 45° to the linea alba). Adhesives were used (adhesive spray, double-sided tape, and cover tape) to prevent any movement of the sensors on the skin. Afterward, a lumbar belt was tightly wrapped around the waist to improve electrode contact and minimize noise. The EMG data was sampled and digitized with a frequency of 2148 Hz, band-pass filtered with a frequency of 20–450 Hz using duo wireless amplifiers and EMGWorks (Delsys Inc. Natick, MA, USA).

EMG processing

EMG data was processed using a custom Matlab (The MathWorks, Natick, MA) code with a zero-lag 4th order band-pass filter (50–450 Hz). A linear envelope was produced by rectifying the corrected EMG data and applying a zero-lag 4th order low-pass filter with a 1 Hz for the MVIC tasks or a 6 Hz cut-off for main blocks. For main blocks, linear envelope signals were time-normalized from 0 to 100% using a quadratic spline interpolation

for each task described in the phase segmentation section. For each muscle, EMG signals were amplitude normalization to peak EMG activity recorded during the MVIC task. Peak and median EMG amplitudes were averaged across back extensors and abdominal muscles for our main statistical analysis. As a primary outcome measure, 95th percentile and 50th percentile back extensor EMG amplitudes were calculated for each phase as a surrogate of peak and median. As a secondary outcome measure, 95th percentile and 50th percentile abdominal EMG amplitudes were calculated for each task.

IMU setup and processing
Inertial measurement units (IMUs) were positioned on the participant's skin on the C7, T8, L1, and S1 spinal process and two additional ones on the posterior thighs (middle of the hamstring) using adhesives (spray, double-sided tape, and cover tape). During the study, IMU data was sampled along with exo IMU data, load cell data, and the devices anticipated force command with a frequency of 200 Hz using an 8-bit microprocessing unit (PIC18F25K80, Microchip Technology, Inc., AZ, USA) and an onboard flash memory card (SDSQUNC-032G-AN6IA, Scandisk, CA, USA). Finally, a custom Matlab code was used to process the angular data of the skin and suit-mounted IMUs, and suit load cell data using a zero-lag 4th order 2 Hz low-pass filter.

Motion capture setup
Motion capture data was recorded using an optical marker-based camera system (Oqus 700, Qualisys™, Göteborg, Sweden). Fifty-eight passive reflective markers were placed on the participants. Sixteen markers were positioned bilaterally on the radial and ulnar styloid, medial and lateral malleolus, medial and lateral femoral epicondyles, greater trochanter, acromion, heel, distal 3rd phalanges, 1st and 5th metatarsal, medial and lateral calcaneus, and the anterior and posterior-anterior iliac spine. Individual passive reflective markers were positioned on the suprasternal notch and the 7th cervical spinous process. Four marker bilateral rigid body clusters were placed on the iliac crests, thighs, and shanks. Following setup, a standing calibration (T-Pose) captured the three-dimensional marker position relative to the rigid bodies using twenty-two infrared emitting cameras sampled at 200 Hz using Qualisys Track Manager. All lifting and lowering tasks of the study were performed while standing on force plates (AM6800, BertecTM, Columbus, OH) sampled at 200 Hz using a ± 5 V using a 16-bit analog-to-digital board (230599, Qualisys™).

Kinematics and kinetics data processing
The motion capture data was collected, labeled, and interpolated using Qualisys Track Manager (Qualisys™, Göteborg, Sweden). Kinematic and kinetic data were post-processed in V3D (Visual3D, C-Motion, Germantown, MD, USA) using a 4th order, 6 Hz low-pass filter. For each participant, overall moments around the ankle, knee, hip, and trunk were calculated using a bottom-up inverse-dynamic approach[23]. All relative angular kinematics and moments in the sagittal plane were time normalized over 400 data points from 0 to 100% using a quadratic spline interpolation for each task. To acquire the biological lumbar moment, a time-normalized suit load cell data was converted to moment, which was then subtracted from the sagittal plane overall moment based on a 0.12 m constant moment arm[60,70]. Mean absolute error (MAE) was calculated between suit load cell data and the suit's expected force command to determine controller accuracy. As a primary outcome measure, 95th and 50th percentile biological lumbar moments were calculated for each phase. The 95th and 50th percentiles of the overall lumbar moment and MAE were calculated for each task as a secondary outcome. Additionally, kinematics measurements, including 95th percentile trunk, hip, knee, and ankle dorsiflexion, were calculated across each task (lifting and lowering[71]) as secondary outcome measures.

Movement phase segmentation
All the biomechanical data were synchronized using a common signal logged by all equipment. They were segmented into four phases or two tasks using the force plate data and the movement data captured by IMUs. The four phases include unweighted flexion, weighted extension, weighted flexion, and unweighted extension, depending on the movement and the weighted status. The flexion phase was defined as the period when the trunk flexion angle exceeds 30°, and the velocity is positive. Similarly, the extension phase was defined as the trunk flexion angle exceeding 30°, with negative velocity. The weighted phase was defined as the normal force on the force plate for the object was less than 10% of the object's weight. Otherwise, it is defined as the unweighted phase. The tasks combine flexion and extension in sequence, i.e., the lifting task is a combination of unweighted flexion and weighted extension, and the lowering task is a combination of weighted flexion and unweighted extension.

Perceptual data - survey questions
We asked four categories of questions to investigate participants' perceptual impressions of the controllers from various perspectives. To probe the negative perceptual impact of controllers, we asked participants how often they felt the assistance was (i) too much, (ii) too little, (iii) jerky, and (iv) restrictive during each controller trial (Table S1). To understand how participants liked the controllers, we asked participants if (i) a controller made lifting easier, (ii) a controller applied the right amount of support, (iii) they were satisfied with the assistance, and (iv) they would like to use it if they would do similar task all day (see complete wording in Table S1). To investigate whether the controllers work adequately for different weights, we asked participants to rate the overall performance of a controller for each weight (Table S2). Participants answered all the questions in Tables S1 & S2 using a seven-point Likert scale. To probe the negative implications of an exosuit controller for unique weights, participants were asked to identify four negative controller properties on a binary scale (Table S3). Participants practiced these questions during familiarization and were cued on what negative attributes to focus

on before starting each main experimental block to increase their confidence in providing answers. Participants' responses were collected using the survey tool presented on a tablet (Qualtrics XM, Provo, UT, USA).

Perceptual data processing

All answers based on a seven-point Likert scale were transferred to a point score from 0 to 6, with low scores designed to quantify poor performance. As a primary outcome measure, we calculated the overall composite score as a holistic performance measure by summing up the scores of all the questions. Average scores were calculated for negative frequency scores and positive attribute scores. Specific questions were considered within the category as a pseudo-post-hoc analysis. Weight satisfaction scores were considered for each weight to probe controller by mass interactions. For the negative binary questions, the presence of a negative attribute was provided with a score of 0. The sum of the four negative binary scores were compared statistically. We normalized the holistic performance scores (overall composite score) from 0 to 100% to compare them on the same scale.

Statistical analysis

The statistical analysis was performed for two data categories (biomechanical and perceptual) using Linear Mixed Model (LLM) ANOVAs with participants as a random factor. For primary biomechanical outcome measures (exosuit assistance and back extensor EMG activity), the model had three factors based on weight (light, medium, heavy), the controller (three controllers & SLACK), the block (first and second), the phase (unweighted flexion, weighted extension, weighted flexion, unweighted extension). Secondary biomechanical outcome measures were included to corroborate findings of biomechanical effectiveness (biological back extensor moments). In this circumstance, study outcomes were analyzed using a similar LMM. Additional secondary biomechanical outcomes were included to describe potential device incompatibility (mean absolute error, abdominal EMG activity, overall lumbar moments, and 95th percentile trunk, hip, knee, and ankle flexion). These secondary LMM included four factors (weight (3), controller (4), block (2), and task (lifting and lowering)). All models were implemented on peak (95th percentile) biomechanical outcomes. However, as a surrogate measure of overall load suit forces, mean absolute error, EMG amplitude spinal moments also modelled median (50th percentile) outcomes.

Perceptual data were derived from multiple questions. For most questions, the perceptual data were compared between the controller and block in a two-factor LMM ANOVA. However, the participants' overall perception of the controller for a specific weight was analyzed in a three-factorial LMM ANOVA (weight, controller, and block). Since perceptual data span multiple questions, our primary perceptual outcome measure was the calculated overall composite perceptual score (Table S1). All other perceptual data points and interactions were considered secondary outcomes to improve the overall understanding of what factors sculpted an individual's device perception.

All statistical models were applied to the questions' respective points or composite scores, while percentages were only used to make the results more understandable. For simplicity, the factor block was removed from all models after preliminary analysis captured no block main effects for primary outcome measures. To correct for multiple (5) primary outcome measures, the interpretation of significant ANOVA main effects and interactions were Bonferroni corrected, considered significant with an alpha of 0.0125. As many secondary outcome measures sought to determine equivalence between controllers (biomechanics) or were exploratory in nature (perception), features were considered significant with a liberal alpha of 0.005. All data were checked for normality. Owing to the small biomechanical differences between exosuit controllers, significant main effects and interactions were analyzed with a Fisher LSD post-hoc using Minitab version 22 (Minitab LLC, PA, USA).

Data availability

The datasets used and/or analyzed during the current study are available from the corresponding author C.J.W upon reasonable request.

Code availability

The code developed to calculate these derivations is available from the corresponding author C.J.W on request.

Received: 13 September 2024; Accepted: 17 March 2025
Published online: 29 March 2025

References

1. Kermavnar, T., de Vries, A. W., de Looze, M. P. & O'Sullivan, L. W. Effects of industrial back-support exoskeletons on body loading and user experience: an updated systematic review. *Ergonomics* **64**, 685–711 (2021).
2. Norman, R. et al. A comparison of peak vs cumulative physical work exposure risk factors for the reporting of low back pain in the automotive industry. *Clin. Biomech.* **13**, 561–573 (1998).
3. Coenen, P. et al. Cumulative low back load at work as a risk factor of low back pain: A prospective cohort study. *J. Occup. Rehabilitation*. **23**, 11–18 (2013).
4. Marras, W. S., Walter, B. A., Purmessur, D., Mageswaran, P. & Wiet, M. G. The contribution of Biomechanical-Biological interactions of the spine to low back pain. *Hum. Factors: J. Hum. Factors Ergon. Soc.* **58**, 965–975 (2016).
5. Marras, W. S., Allread, W. G., Burr, D. L. & Fathallah, F. A. Prospective validation of a low-back disorder risk model and assessment of ergonomic interventions associated with manual materials handling tasks. *Ergonomics* **43**, 1866–1886 (2000).
6. Zelik, K. E. et al. An ergonomic assessment tool for evaluating the effect of back exoskeletons on injury risk. *Appl. Ergon.* **99**, 103619 (2022).
7. Natali, C. D., Buratti, G., Dellera, L. & Caldwell, D. Equivalent weight: application of the assessment method on real task conducted by railway workers wearing a back support exoskeleton. *Appl. Ergon.* **118**, 104278 (2024).
8. Ahmad, J., Fanti, V., Caldwell, D. G. & Natali, C. D. Framework for the adoption, evaluation and impact of occupational exoskeletons at different technology readiness levels: A systematic review. *Robot Auton. Syst.* **179**, 104743 (2024).

9. Baldassarre, A. et al. Industrial exoskeletons from bench to field: Human-machine interface and user experience in occupational settings and tasks. *Front. Public. Heal.* **10**, 1039680 (2022).
10. Kuber, P. M., Abdollahi, M., Alemi, M. M. & Rashedi, E. A systematic review on evaluation strategies for field assessment of Upper-Body industrial exoskeletons: current practices and future trends. *Ann. Biomed. Eng.* **50**, 1203–1231 (2022).
11. Näf, M. B. et al. Passive back support exoskeleton improves range of motion using flexible beams. *Front. Robot AI.* **5**, 72 (2018).
12. Matijevich, E. S., Volgyesi, P. & Zelik, K. E. A promising wearable solution for the practical and accurate monitoring of low back loading in manual material handling. *Sensors* **21**, 340 (2021).
13. Yuan, R., Wang, Q., Xu, H., Yu, H. & Shi, P. Control strategies for trunk exoskeletons based on motion intent recognition: A review. *NeuroRehabilitation* **54**, 575–597 (2024).
14. Abdoli-E, M., Agnew, M. J. & Stevenson, J. M. An on-body personal lift augmentation device (PLAD) reduces EMG amplitude of erector spinae during lifting tasks. *Clin. Biomech.* **21**, 456–465 (2006).
15. Frost, D. M., Abdoli-E, M. & Stevenson, J. M. PLAD (personal lift assistive device) stiffness affects the lumbar flexion/extension moment and the posterior chain EMG during symmetrical lifting tasks. *J. Electromyogr. Kinesiol.* **19**, e403–e412 (2009).
16. Toxiri, S. et al. Rationale, implementation and evaluation of assistive strategies for an active Back-Support exoskeleton. *Front. Robot AI.* **5**, 53 (2018).
17. Koopman, A. S., Kingma, I., de Looze, M. P. & van Dieën, J. H. Effects of a passive back exoskeleton on the mechanical loading of the low-back during symmetric lifting. *J. Biomech.* **102**, 109486 (2020).
18. Baltrusch, S. J., van Dien, J. H., van Bennekom, C. A. M. & Houdijk, H. Testing an exoskeleton that helps workers with Low-Back pain. *IEEE Robot Autom. Mag.* **27**, 66–76 (2020).
19. Toxiri, S. et al. Back-Support exoskeletons for occupational use: an overview of technological advances and trends. *IISE Trans. Occup. Ergon. Hum. Factors.* **7**, 237–249 (2019).
20. Poliero, T. et al. Versatile and non-versatile occupational back-support exoskeletons: A comparison in laboratory and field studies. *Wearable Technol.* **2**, e12 (2021).
21. Goršič, M., Song, Y., Dai, B. & Novak, D. Evaluation of the HeroWear apex back-assist exosuit during multiple brief tasks. *J. Biomech.* **126**, 110620 (2021).
22. Engelhoven, L. V. et al. Experimental evaluation of a Shoulder-Support exoskeleton for overhead work: influences of peak torque amplitude, task, and tool mass. *IISE Trans. Occup. Ergon. Hum. Factors.* **7**, 250–263 (2019).
23. Quirk, D. A. et al. Evaluating adaptiveness of an active back exosuit for dynamic lifting and maximum range of motion. *Ergonomics* **67**, 660–673 (2023).
24. Kim, S., Madinei, S., Alemi, M. M., Srinivasan, D. & Nussbaum, M. A. Assessing the potential for undesired effects of passive back-support exoskeleton use during a simulated manual assembly task: muscle activity, posture, balance, discomfort, and usability. *Appl. Ergon.* **89**, 103194 (2020).
25. Sänger, J. et al. Evaluation of active shoulder exoskeleton support to deduce Application-Oriented optimization potentials for overhead work. *Appl. Sci.* **12**, 10805 (2022).
26. Ramella, G. et al. Evaluation of antigravitational support levels provided by a passive upper-limb occupational exoskeleton in repetitive arm movements. *Appl. Ergon.* **117**, 104226 (2024).
27. Fick *Use of acceptability and usability trials to evaluate various design iterations of the Personal Lift Assistive Device* (Queen's University, Kingston, 2012).
28. Hensel, R. & Keil, M. Subjective Evaluation of a Passive Industrial Exoskeleton for Lower-back Support: A Field Study in the Automotive Sector. *IISE Trans. Occup. Ergon. Hum. Factors.* **7**, 213–221 (2019).
29. Elprama, S. A., Vanderborght, B. & Jacobs, A. An industrial exoskeleton user acceptance framework based on a literature review of empirical studies. *Appl. Ergon.* **100**, 103615 (2022).
30. Lazzaroni, M. et al. Control of a Back-Support Exoskeleton to Assist Carrying Activities. *2023 Int. Conf. Rehabilitation Robot (ICORR).* **00**, 1–6 (2023).
31. Natali, C. D., Poliero, T., Fanti, V., Sposito, M. & Caldwell, D. G. Dynamic and Static Assistive Strategies for a Tailored Occupational Back-Support Exoskeleton: Assessment on Real Tasks Carried Out by Railway Workers. *Bioengineering* **11**, 172 (2024).
32. Divekar, N. V., Thomas, G. C., Yerva, A. R., Frame, H. B. & Gregg, R. D. A versatile knee exoskeleton mitigates quadriceps fatigue in lifting, lowering, and carrying tasks. *Sci. Robot.* **9**, eadr8282 (2024).
33. Molinaro, D. D. et al. Task-agnostic exoskeleton control via biological joint moment estimation. *Nature* **635**, 337–344 (2024).
34. Molinaro, D. D., Kang, I. & Young, A. J. Estimating human joint moments unifies exoskeleton control, reducing user effort. *Sci. Robot.* **9**, eadi8852 (2024).
35. Lazzaroni, M. et al. Acceleration-based Assistive Strategy to Control a Back-support Exoskeleton for Load Handling: Preliminary Evaluation. *IEEE 16th Int. Conf. Rehabilitation Robot. (ICORR)* 00, 625–630 (2019). (2019).
36. Chung, J. et al. Lightweight active back exosuit reduces muscular effort during an hour-long order picking task. *Commun. Eng.* **3**, 35 (2024).
37. Li, J. M. et al. Design and Validation of a Cable-Driven Asymmetric Back Exosuit. *IEEE Trans. Robot.* **38**, 1489–1502 (2022).
38. Johns, J., Schultes, I., Heinrich, K., Potthast, W. & Glitsch, U. Biomechanical analysis of different back-supporting exoskeletons regarding musculoskeletal loading during lifting and holding. *J. Biomech.* **168**, 112125 (2024).
39. Lazzaroni, M. et al. Improving the Efficacy of an Active Back-Support Exoskeleton for Manual Material Handling Using the Accelerometer Signal. *IEEE Robot Autom. Lett.* **7**, 7716–7721 (2022).
40. Li, J. et al. Development and Evaluation of a Lumbar Assisted Exoskeleton With Mixed Lifting Tasks by Various Postures. *IEEE Trans. Neural Syst. Rehabilitation Eng.* **31**, 2111–2119 (2023).
41. Arens, P., Quirk, D. A. & Walsh, C. J. Deep-Learning Lumbar Moment Estimation during Back Exosuit Augmented Lifting with Variable Loading Conditions. ,*10th IEEE RAS/EMBS International Conference for Biomedical Robotics and Biomechatronics (BioRob)* (2024). (2024).
42. Moya-Esteban, A., Sridar, S., Refai, M. I. M., Kooij, H. & Sartori, M. Adaptive Assistance with an Active and Soft Back-Support Exosuit to Unknown External Loads via Model-Based Estimates of Internal Lumbosacral Moments. *arXiv* https://doi.org/10.48550/arxiv.2311.01843 (2023).
43. Missiroli, F. et al. Integrating Computer Vision in Exosuits for Adaptive Support and Reduced Muscle Strain in Industrial Environments. *IEEE Robot Autom. Lett.* **9**, 859–866 (2023).
44. Zhang, T. & Huang, H. H. A Lower-Back Robotic Exoskeleton. *IEEE Robot Autom. Mag.* **25**, 95–106 (2018).
45. Saito, Y. et al. Efficacy of exercise with the hybrid assistive limb lumbar type on physical function in mobility-limited older adults: A 5-week randomized controlled trial. *Exp. Gerontol.* **195**, 112536 (2024).
46. Yasunaga, Y. et al. Biofeedback Physical Therapy With the Hybrid Assistive Limb (HAL) Lumbar Type for Chronic Low Back Pain: A Pilot Study. *Cureus* **14**, e23475 (2022).
47. Khamaisi, R. K. et al. A multi-facet approach to functional and ergonomic assessment of passive exoskeletons. *Procedia Comput. Sci.* **232**, 584–594 (2024).
48. Hess, A. et al. Active back exosuits demonstrate positive usability perceptions that drive intention-to-use in the field among logistic warehouse workers. *Appl. Ergon.* **122**, 104400 (2025).
49. Nasr, A., Hunter, J., Dickerson, C. R. & McPhee, J. Evaluation of a machine-learning-driven active–passive upper-limb exoskeleton robot: Experimental human-in-the-loop study. *Wearable Technol.* **4**, e13 (2023).

50. Pesenti, M. et al. IMU-based human activity recognition and payload classification for low-back exoskeletons. *Sci. Rep.* **13**, 1184 (2023).
51. Peters, S. L. A., Tabasi, A., Kingma, I., van Dijk, W. & van Dieën, J. H. Development of a real time estimation method of L5S1 moments in occupational lifting. *J. Biomech.* **146**, 111417 (2023).
52. Okunola, A., Afolabi, A., Akanmu, A., Jebelli, H. & Simikins, S. Facilitators and barriers to the adoption of active back-support exoskeletons in the construction industry. *J. Saf. Res.* **90**, 402–415 (2024).
53. Lamers, E. P., Yang, A. J. & Zelik, K. E. Feasibility of a Biomechanically-Assistive Garment to Reduce Low Back Loading During Leaning and Lifting. *IEEE Trans. Biomed. Eng.* **65**, 1674–1680 (2018).
54. McFarland, T. C., McDonald, A. C., Whittaker, R. L., Callaghan, J. P. & Dickerson, C. R. Level of exoskeleton support influences shoulder elevation, external rotation and forearm pronation during simulated work tasks in females. *Appl. Ergon.* **98**, 103591 (2022).
55. Jackson, R. W. & Collins, S. H. An experimental comparison of the relative benefits of work and torque assistance in ankle exoskeletons. *J. Appl. Physiol.* **119**, 541–557 (2015).
56. Verdel, D., Bruneau, O., Sahm, G., Vignais, N. & Berret, B. The value of time in the invigoration of human movements when interacting with a robotic exoskeleton. *Sci. Adv.* **9**, eadh9533 (2023).
57. Hybart, R. L. & Ferris, D. P. Embodiment for Robotic Lower-Limb Exoskeletons: A Narrative Review. *IEEE Trans. Neural Syst. Rehabilitation Eng.* **31**, 657–668 (2023).
58. de Looze, M. P., Toussaint, H. M., van Dieën, J. H. & Kemper, H. C. G. Joint moments and muscle activity in the lower extremities and lower back in lifting and lowering tasks. *J. Biomech.* **26**, 1067–1076 (1993).
59. Willoughby, D. S. & Taylor, L. Effects of concentric and eccentric muscle actions on serum myostatin and follistatin-like related gene levels. *J. sports Sci. Med.* **3**, 226–233 (2004).
60. Quirk, D. A. et al. Reducing Back Exertion and Improving Confidence of Individuals with Low Back Pain with a Back Exosuit: A Feasibility Study for Use in BACPAC. *Pain Med. : Off J. Am. Acad. Pain Med.* **24**, S175–S186 (2023).
61. Yun, S. S., Kim, K., Ahn, J. & Cho, K. J. Body-powered variable impedance: An approach to augmenting humans with a passive device by reshaping lifting posture. *Sci. Robot.* **6**, eabe1243 (2021).
62. Babič, J. et al. Challenges and solutions for application and wider adoption of wearable robots. *Wearable Technol.* **2**, e14 (2021).
63. Lee, C. J. & Lee, J. K. Inertial Motion Capture-Based Wearable Systems for Estimation of Joint Kinetics: A Systematic Review. *Sensors* **22**, 2507 (2022).
64. Molinaro, D. D. et al. Subject-Independent, Biological Hip Moment Estimation During Multimodal Overground Ambulation Using Deep Learning. *IEEE Trans. Méd Robot Bionics.* **4**, 219–229 (2022).
65. Arens, P. et al. Preference-Based Assistance Optimization for Lifting and Lowering with a Soft Back Exosuit. *Sci. Advances* (2024).
66. Ludvig, D. & Larivière, C. Trunk muscle reflexes are elicited by small continuous perturbations in healthy subjects and patients with low-back pain. *J. Electromyogr. Kinesiol.* **30**, 111–118 (2016).
67. He, K., Zhang, X., Ren, S. & Sun, J. Deep Residual Learning for Image Recognition. *2016 IEEE Conf. Comput. Vis. Pattern Recognit. (CVPR).* **770-778** https://doi.org/10.1109/cvpr.2016.90 (2016).
68. Deng, J. et al. ImageNet: A large-scale hierarchical image database. *2009 IEEE Conf. Comput. Vis. Pattern Recognit.* **248–255** https://doi.org/10.1109/cvpr.2009.5206848 (2009).
69. Winter, D. A. Biomechanics and Motor Control of Human Movement. 82–106 (2010). https://doi.org/10.1002/9780470549148.ch4
70. Banks, J. J. et al. The effect of a soft active back support exosuit on trunk motion and thoracolumbar spine loading during squat and stoop lifts. *Ergon.* **68**(2), 223–236. https://doi.org/10.1080/00140139.2024.2320355 (2025).
71. Lamers, E. P. & Zelik, K. E. Design, modeling, and demonstration of a new dual-mode back-assist exosuit with extension mechanism. *Wearable Technol.* **2**, e1 (2021).

Acknowledgements

We thank Philipp Arens and Marija Bakoc for their contributions to this work, the participants who volunteered for this study, and Sarah Sullivan from the Wyss Institute Clinical Research team.

Author contributions

Conceptualization: JC, DAQ, CJWDevelopment: JC, DAQ, DKProtocol design: JC DAQ, JMC, DF, DK, CJW-Data collection: JC, DAQ, JMC, DFData analysis: JC, DAQ, JMC, DFFunding acquisition: JC, DAQ, CWWriting – original draft: JC, DAQ, JMC, DF, DK, CJWWriting – review & editing: JC, DAQ, CJW.

Funding

This work was supported by NIH BACPAC grants 1UH2AR076731-01 (CJW). DOD grant W81XWH2010609 (CJW). Harvard University John A. Paulson School of Engineering and Applied Sciences. Wyss Institute for Biologically Inspired Engineering. Boston University Sargent College of Health & Rehabilitation Science.

Declarations

Ethics approval and consent to participate

All participants were provided with and signed informed consent approved by the Harvard Medical School's Institutional Review Board (IRB18-0960).

Competing interests

C.J.W. & J.C., are inventors of at least one patent application describing the exosuit components described in the paper that have been filed with the U.S. Patent Office by Harvard University. Harvard University has entered into a licensing agreement with Verve Inc., in which C.J.W. & J.C., have an equity interest, and C.J.W. has a board positions. The other authors declare that they have no competing interests.

Additional information

Supplementary Information The online version contains supplementary material available at https://doi.org/10.1038/s41598-025-94726-3.

Correspondence and requests for materials should be addressed to J.C. or C.J.W.